Bulletin of the Geological Society of Finland, Vol. 88, 2016, pp 5–20, http://dx.doi.org/10.17741/bgsf/88.1.001

New monazite U-Pb age constraints on the evolution of the Paleoproterozoic Vaasa granitoid batholith, western Finland

VERTAISARVIOITU
KOLLEGIALT GRANSKAD
PEER-REVIEWED
www.tsv.fi/tunnus

Anna K. Kotilainen[1*], Irmeli Mänttäri[2], Matti Kurhila[2], Pentti Hölttä[2] and O. Tapani Rämö[1]

[1] *Department of Geosciences and Geography, Division of Geology and Geochemistry (DiGG), P.O. Box 64, FI-00014 University of Helsinki, Finland*

[2] *Geological Survey of Finland, P.O. Box 96, FI-02151 Espoo, Finland*

Abstract

The Vaasa batholith, western Finland, is a large, peraluminous granitoid pluton that crystallized at 1.88–1.87 Ga during the culmination of the Svecofennian orogeny. The batholith has gradual contacts, through metatexites and diatexites, with the enveloping metasedimentary rocks of the Bothnian Belt. We present ID-TIMS U-Pb age data on monazite from granitoids and xenoliths of the Vaasa batholith and combine these with published U–Pb zircon ages in order to shed further light on the evolution of the Vaasa batholith. The apparent monazite ages for seven of the examined samples are 1870–1863 Ma, and 1855±3 Ma for one further sample from the southern part of the batholith. Combined with pre-existing data, the monazite ages of the granitoids are 9 to 18 Ma (face values) or 3 to 9 Ma (external errors considered) younger than the U–Pb zircon crystallization ages from respective samples. Our new data suggest slow cooling for the Vaasa batholith – the closure/saturation temperature of the monazite U–Pb system was probably reached in ~10 m.y. after the crystallization of magmatic zircon in the examined rocks.

Keywords: monazite, U–Pb geochronology, anatexis, granitoid, Svecofennian, Vaasa, Finland

*Corresponding author e-mail: anna.kotilainen@helsinki.fi

Editorial handling: Jussi S. Heinonen (jussi.s.heinonen@helsinki.fi)

1. Introduction

The Svecofennian orogeny has been actively studied utilizing the U-Th-Pb system in zircon and further isotope geochemical methods (e.g., Kouvo & Tilton, 1966; Patchett et al., 1981; Vaasjoki, 1981; Huhma, 1986) as well as tectonic modelling (e.g., Nironen, 1997; Lahtinen et al., 2005; 2009). The growth of the Svecofennian orogen was probably related to collisional and extensional events in which several crustal terranes were accreted, at 1.92–1.79 Ga, to the Archean Karelian craton (e.g., Nironen, 1997; Lahtinen et al., 2005; 2009; Korja & Heikkinen, 2005). Detailed temporal history of the various evolutionary stages of the Svecofennian orogeny is yet to be determined, however. In order to further understand the magmatism related to the Svecofennian orogeny in Finland, the Vaasa batholith – a prominent Svecofennian granitoid pluton in western Finland surrounded by metasedimentary rocks and having been formed during the culmination of the Svecofennian orogeny at 1.90–1.87 Ga (e.g., Lahtinen et al., 2005) – has been studied. There is no unanimous consensus on the origin of the Vaasa batholith. It has been interpreted as entirely diatexitic (Lahtinen et al. 2005), proposed to represent a metamorphic core complex (Valtonen, 2011; Hölttä, 2013), and the result of *in situ* melting of the Bothnian Belt metasedimentary rocks (Mäkitie, 2001; Sipilä et al., 2008; Mäkitie et al., 2012). Mäkitie et al. (2012) further suggested that the grainitoids of Vaasa batholith represent a 'magma layer', not accumulated melting products of migmatite protoliths.

U–Pb zircon geochronology, tectonic evolution, and chemical composition of the Vaasa batholith have been studied rather extensively (e.g., Lehtonen et al., 2005; Sipilä et al., 2008; Suikkanen et al., 2014; Kotilainen et al., 2016). However, U-Pb monazite chronology of the Vaasa granite has not been thoroughly examined. Monazite, a LREE (light rare earth element) phosphate, is a common accessory mineral in granitoid rocks and a useful U–Pb dating proxy, because it has abundant Th and U and low initial common Pb (Parrish, 1990). Monazite crystallizes from metaluminous and peraluminous granitic melts (e.g., Parrish, 1990). In contrast to zircon, inheritance in monazite is not common (e.g., Copeland et al., 1988; Parrish, 1990) and monazite is also comparatively resistant to Pb loss (Smith & Giletti, 1997; Cherniak et al., 2004). Hence, monazite can be used to date the crystallization of magmatic rocks (e.g., Parrish, 1990; Noble & Searle, 1995). In this regard, issues may arise from age zoning (e.g., Parrish, 1990; Williams et al., 1999), deformation (e.g., Vavra & Schaltegger, 1999; Krohe & Wawrzenitz, 2000) and/or fluid induced recrystallization (Teufel & Heinrich, 1997; Townsend et al., 2000).

In this paper, we present new ID-TIMS (Isotopic Dilution Thermal Ionization Mass Spectrometry) U–Pb data on multi-grain monazite fractions from granitoids and xenoliths of the Vaasa batholith. Assessment of these results in comparison to published U–Pb zircon data sheds further light on the temporal evolution of the Vaasa batholith and history of the Svecofennian orogen.

2. Geologic setting

The Bothnian Belt, which governs the western part of the Svecofennian orogeny in Finland, was formed when the supracrustal sequences of the basin were metamorphosed at 1.89–1.88 Ga (Kähkönen, 2005) during the culmination of the Svecofennian orogeny. The belt consists of turbiditic metagraywackes, mica gneisses, and mica schists, which were formed in low-P amphibolite facies conditions (Kähkönen, 2005), and includes a prominent, 1.88–1.86 Ga multi-phase granitoid area, the Vaasa batholith (Fig. 1; e.g., Lundqvist & Autio, 2000; Mäkitie et al., 2012). The batholith, together with the surrounding metasediments, comprises the Vaasa complex. The boundary between the granitoids of the Vaasa batholith and the schists of the Bothnian Belt is gradual through metatexites and diatexites (Mäkitie et al., 2012) with no observed intrusive contacts (Mäkitie et al.,

1999; Mäkitie, 2001; Lehtonen et al., 2005; Sipilä et al., 2008). In fact, the boundary area is texturally, mineralogically, and geochemically continuous (Mäkitie et al., 2012). This has led many workers to consider the granitoids of the Vaasa complex to represent *in situ* melting (e.g., Mäkitie, 2001; Sipilä et al., 2008; Mäkitie et al., 2012).

The Vaasa batholith consists of four granitoid groups: porphyritic granodiorite, even-grained granodiorite, pyroxene granitoids (tonalites and granodiorites), and granites *sensu stricto* (Mäkitie et al., 2012). Also, small areas of tonalite are found near the border of the batholith. Granodiorites are the most common rock type in the Vaasa batholith. They are typically coarse-grained, slightly inhomogeneous and weakly foliated, and they often contain inclusions. Porphyritic and even-grained granodiorites are occasionally difficult to distinguish as the size and amount of the phenocrysts vary and the contacts are gradual. The mineralogical composition of a typical porphyritic granodiorite from the Vaasa batholith is 29–39% plagioclase, 27–37% quartz, 14–24% biotite, and 7–17% alkali feldspar (Mäkitie et al., 2012). Granites are found in three large areas (Fig. 1) and vary from porphyritic to even-grained and contain inclusions of garnet. Pyroxene granitoids are known but rare. Schist inclusions, calc-silicate xenoliths, and Al-rich accessory minerals are common in the Vaasa batholith (e.g., Lehtonen et al., 2005; Sipilä et al., 2008). Garnet is common in the granitoids in southern parts of the batholith, sparse in the northern parts (Suikkanen et al., 2014).

The granitoids of the Vaasa batholith are peraluminous and were crystallized at 1.88–1.86 Ga according to U–Pb zircon ages thus far published (e.g., Sipilä et al., 2008; Suikkanen et al., 2014; Kotilainen et al., 2016). The maximum sedimentation age of the xenoliths from the Vaasa batholith is ≤ 1.92 Ga (Kotilainen et al., 2016) and is equivalent to the ≤ 1.92–1.91 Ga maximum sedimentation age of the adjacent Bothnian Belt (Lahtinen et al., 2002). Detrital zircon age patterns of the xenoliths in the Vaasa batholith (Kotilainen et al., 2016) are similar to the patterns of previously dated detrital zircon from Svecofennian metasedimentary rocks (cf. Huhma et al., 1991; Claesson et al., 1993; Lahtinen et al., 2002, 2009; Rutland et al., 2004; Bergman et al., 2008). Previous U–Pb monazite analyses of the Vaasa batholith have yielded ages between 1872 and 1858 Ma (Alviola et al., 2001; Sipilä et al., 2008).

3. Samples and analytical methods

The monazite samples are from granitoid-xenolith pairs collected from the main body of Vaasa batholith for U–Pb zircon dating (Kotilainen et al., 2016). From the nine sample pairs collected, six granitoids and two xenoliths had sufficient amount of monazite for U–Pb analysis. Sampling site locations are shown in Fig. 1 and monazite descriptions are in Table 1. For lithologic photographs and petrographic descriptions, see Kotilainen et al. (2016).

Approximately 1–3 kg of each sample was crushed in a jaw crusher and foreign material was removed from the crushed material. Material was ground using a swing mill. The outcome was sieved with a 350 μm sieve and fine dust was washed out. The dried grains were separated by density with di-iodomethane (ρ = 3.3 g/ml) and Clerici solution (ρ = 3.8 g/ml). Magnetic minerals were separated from nonmagnetic and paramagnetic minerals by hand magnet and Frantz magnetic separator. Sulphides were removed from some of the samples using HNO_3. For the U–Pb isotope dilution thermal ionisation mass spectrometry (ID-TIMS) analyses, the monazite grains were hand-picked under the stereomicroscope. Generally, euhedral, translucent to transparent grains were prioritized. Monazite was analyzed using a slightly modified method of that described by Krogh (1973, 1982). The spiked (^{235}U–^{206}Pb) and unspiked isotope ratios were measured with a VG Sector 54 thermal ionisation multicollector mass spectrometer at the Geological Survey of Finland, Espoo. Based on repeated measurements of the SRM981 Pb

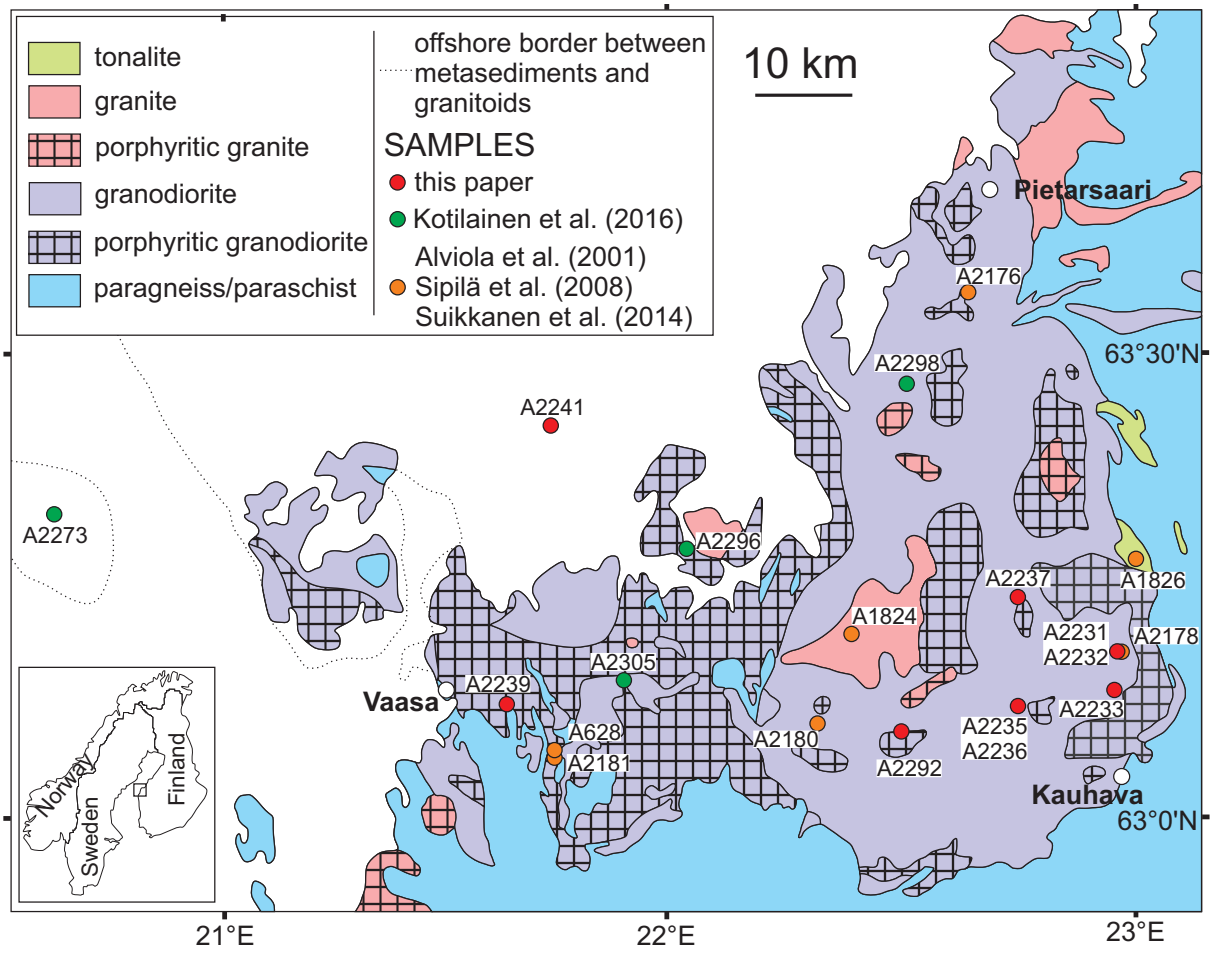

Figure 1. Geological map of the Vaasa batholith, western Finland, based on a 1:200k bedrock map published by the Geological Survey of Finland (Suomen kallioperä, DigiKP200, 1:200 000 kallioperäkartta). Sample sites of this paper, as well as those in Alviola et al. (2001), Sipilä et al. (2008), Suikkanen et al. (2014) and Kotilainen et al. (2016), are marked. Inset shows location of the Vaasa batholith relative to Fennoscandia.

standard, the measured Pb isotopic ratios were corrected for 0.10±0.05 % / a.m.u fractionation. Pb/U ratios were calculated using the PbDat program (Ludwig, 1993) with an age-related common lead correction based on the model of Stacey & Kramers (1975). Data were plotted using ISOPLOT/Ex program (Ludwig, 2012). Age errors are calculated and plotted at 2σ level, decay constant errors are ignored. Whole-rock geochemical data on seven granitoid-xenolith pairs were acquired by the XRF and ICP/MS methods at Labtium Oy and A-Labs (U.S. Geological Survey, Denver, U.S.A.). Sample locations are shown in Fig. 1. In Labtium analyses, quality control sample values were reproduced to within 5 % error on major elements, except for Al_2O_3, where the error was ~10 %. On trace elements, the quality control sample values were reproduced to better than 20 % accuracy, excluding Hf, which does not dissolve completely in HF-$HClO_4$ digestion, and thus yields unrealistically low concentrations.

Table 1. Monazite descriptions, monazite age results, zircon age results of corresponding granitoids (Kotilainen et al., 2016), and age difference between zircon and monazite with and without considering analytical errors. For sample site photographs, and sample and thin section descriptions, see Kotilainen et al. (2016).

Sample Number	Rock Type	Monazite	Zircon age result (Kotilainen et al. 2016)	Monazite age result ($^{206}Pb/^{207}Pb$ age, ID-TIMS)	Age difference between monazite and zircon[(a)]	Location (ETRS-TM35FIN)
A2231 Susivuori#1	Granodiorite	Turbid, subhedral with some fragments, various sizes (small to large). (Fraction: d > 3.6, nonmagn. 0.6 A.)	1881 ± 4 Ma	1870 ± 4 (turbid)	11 Ma (without errors) 3 Ma (with errors)	N: 7014537 E: 300548
A2232 Susivuori#2	Xenolith	Translucent, subhedral and some fragments, medium size most common. (Fraction: d > 3.3, nonmagn. 0.4 A.)		1866 ± 15 (translucent)	*15 Ma (without errors)* *-4 Ma (with errors)*	
A2233 Haudankalliot#1	Granite	Translucent, medium size, mainly subhedral, also a few fragments. (Fraction: d > 3.3, nonmagn. 0.4 A.)	1877 ± 4 Ma	1868 ± 2 (translucent)	9 Ma (without errors) 3 Ma (with errors)	N: 7011233 E: 300586
A2235 Saarineva#1	Granite		1871 ± 5 Ma			N: 7010979 E: 286614
A2236 Saarineva#2	Xenolith	Small, translucent, subhedral and some fragments, mainly pale yellow. (Fraction: d > 3.3, fr.m. 0.6 A.)		1863 ± 3 (translucent)	*8 Ma (without errors)* *0 Ma (with errors)*	
A2237 Hanhimäki#1	Granite	Translucent, medium size and few larger ones, fragments and moderately subhedral. (Fraction: d > 3.3, nonmagn. 0.4 A.)	1873 ± 4 Ma	1864 ± 2 (translucent)	9 Ma (without errors) 3 Ma (with errors)	N: 7020477 E: 290356
A2239 Tallmossen#1	Quartz monzonite	Turbid to transparent, smal ones subhedral, medium to large ones mainly fragments. (Fraction: d > 3.3, fr.m. 1.4 A.)	1883 ± 7 Ma	1865 ± 2 (turbid to transparent)	18 Ma (without errors) 9 Ma (with errors)	N: 7011399 E: 235683
A2241 Långbådan#1	Granodiorite	Small, mainly turbid with small amounts of translucent and transparent, subhedral and some fragments. (Fraction: d > 3.3, fr.m. 0.6 A.)	1877 ± 5 Ma	1863 ± 2 (turbid to transparent)	14 Ma (without errors) 7 Ma (with errors)	N: 7046411 E: 239434
A2292 Frakanin-kalliot#1	Granite	Mainly translucent, subhedral and fragments, medium-size, pale yellow. (Fraction: d > 3.3, fr.m. 0.6 A.)	1872 ± 8 Ma	1855 ± 3 (translucent)	17 Ma (without errors) 6 Ma (with errors)	N: 7006945 E: 277568

(a) The monazite age is compared to the crystallization age of the granitoid. The age difference with errors is the minimum age difference. Age differences between monazites of the xenolith and the zircons of the host granitoids are in italic. Negative values signify overlapping ages.

4. Results

The results of our U–Pb ID-TIMS analyses of monazite from six granitoids and two xenoliths from the Vaasa batholith are shown in Table 2. As the U–Pb data from some of the samples show minor reverse or normal discordance, we were not able to calculate U–Pb concordia ages for all the samples. Therefore, we use $^{207}Pb/^{206}Pb$ ages (Fig. 2) as a proxy for the closure of the U-Pb system in the analyzed monazites. Apart from one sample (the 1855±3 Ma Frakaninkalliot granite), the $^{207}Pb/^{206}Pb$ ages (face values) of these samples are between 1863 and 1870 Ma (n = 7; Långbådan 1863±2 Ma, Hanhimäki 1864±2 Ma, Talmossen 1865±2 Ma, Haudankalliot 1868±2 Ma, Susivuori 1870±4 Ma from granitoid samples, and Saarineva 1863±3 Ma and Susivuori 1866±15 Ma from xenoliths). Except for the Susivuori xenolith, the 1870–1863 Ma group shows very little variation with only a 1-m.y. minimum age gap between the 1863±2 Ma Långbådan granitoid, and the 1870±4 Ma Susivuori and 1868±2 Ma Haudankalliot granitoids.

The monazite ages of the granitoids and the xenoliths do not show significant differences. These results are in accordance with the monazite ages from previous studies on granitoids from the Vaasa batholith area: 1872±5 Ma from a granodiorite (Alviola et al., 2001) 1858±2 and 1865±2 Ma from a granite and tonalite (Sipilä et al., 2008). The anomalously young monazite age from Frakaninkalliot (sample A2292) may indicate existing younger monazite domains and therefore the ID-TIMS result might show a mixed age.

The chemical composition of seven granitoid-xenolith pairs from the Vaasa batholith are shown in Fig. 3 and Table 3. Overall, the granitoid rocks are strongly peraluminous (Fig. 3A) and magnesian (Fig. 3B) granodiorites. They have moderately fractionated REE patterns with pronounced negative Eu anomalies (Fig. 3C). The heavy REEs show more variation than the light REEs. The xenoliths show the same extent of Al saturation as the granitoids (Fig. 3A) and are also magnesian (Fig. 3B), but show less pronounced REE fractionation with higher overall heavy REE contents compared to the granitoids (Fig. 3C).

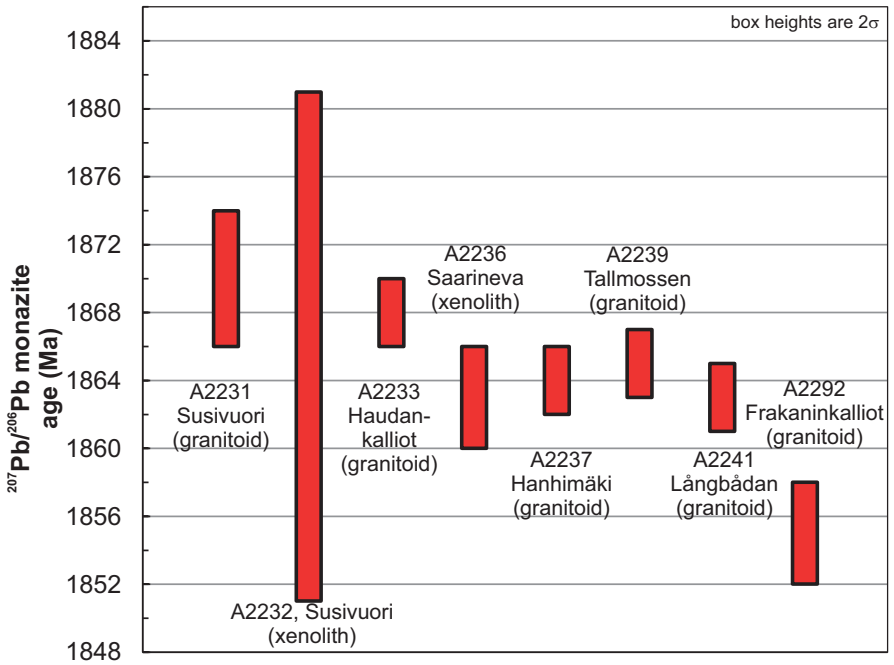

Figure 2. $^{207}Pb/^{206}Pb$ ages of eight monazite fractions analyzed from six granitoids and two xenoliths from the Vaasa batholith. For sample identity, see Table 3.

Table 2. Multigrain ID-TIMS monazite U-Pb isotopic data for five granitoids, a quartz monzonite, and two xenoliths from the Vaasa batholith.

Sample information	Sample	U	Pb	$^{206}Pb/^{204}Pb$	$^{208}Pb/^{206}Pb$	ISOTOPIC RATIOS[b]						Rho[c]	APPARENT AGES/Ma±2σ		
Analysed mineral and fraction [a]	mg	ppm		measured	radiogenic	$^{206}Pb/^{238}U$	±2σ%	$^{207}Pb/^{235}U$	±2σ%	$^{207}Pb/^{206}Pb$	±2σ%		$^{206}Pb/^{238}U$	$^{207}Pb/^{235}U$	$^{207}Pb/^{206}Pb$
A2231 Susivuori, granodiorite															
monazite, turbid	0,54	1784	5339	30374	4,49	0,3372	0,90	5,317	0,91	0,1144	0,178	0,98	1873	1872	1870±4
A2232 Susivuori, xenolith															
monazite, translucent	0,71	850	2293	21739	8,08	0,3384	0,91	5,325	1,24	0,1141	0,831	0,74	1879	1873	1866±15
A2233 Haudankalliot, granite															
monazite, translucent	0,73	2870	5175	29210	4,91	0,3456	1,06	5,445	1,06	0,1143	0,0776	1,00	1914	1892	1868±2
A2236 Saarineva, xenolith															
monazite, translucent	0,48	1979	3551	24579	5,21	0,3276	0,92	5,147	0,94	0,1139	0,159	0,99	1827	1844	1863±3
A2237 Hanhimäki, granite															
monazite, translucent	0,46	3473	4421	19611	3,24	0,3376	0,97	5,307	0,98	0,1140	0,0909	1,00	1875	1870	1864±2
A2239 Tallmossen, quartz monzonite															
monazite, turbid to transparent	0,62	2210	4222	16700	5,45	0,3357	0,97	5,281	0,98	0,1141	0,111	0,99	1866	1866	1865±2
A2241 Långbådan, granodiorite															
monazite, turbid to transparent	0,61	4760	4584	18940	2,34	0,3220	1,31	5,059	1,32	0,1139	0,0887	1,00	1800	1829	1863±2
A2292 Frakaninkalliot, granite															
monazite, translucent	0,44	1241	1910	29210	4,06	0,3425	0,89	5,355	0,90	0,1134	0,143	0,99	1899	1878	1855±3

a) Monazites abraded 15 minutes.

b) Isotopic ratios corrected for fractionation, blank (50 pg), and age related common lead (Stacey & Kramers 1975; $^{206}Pb/^{204}Pb$±0.2, $^{207}Pb/^{204}Pb$±0.1, $^{208}Pb/^{204}Pb$±0.2).

c) Rho: Error correlation between $^{206}Pb/^{238}U$ and $^{207}Pb/^{235}U$ ratios. All errors are 2 sigma.

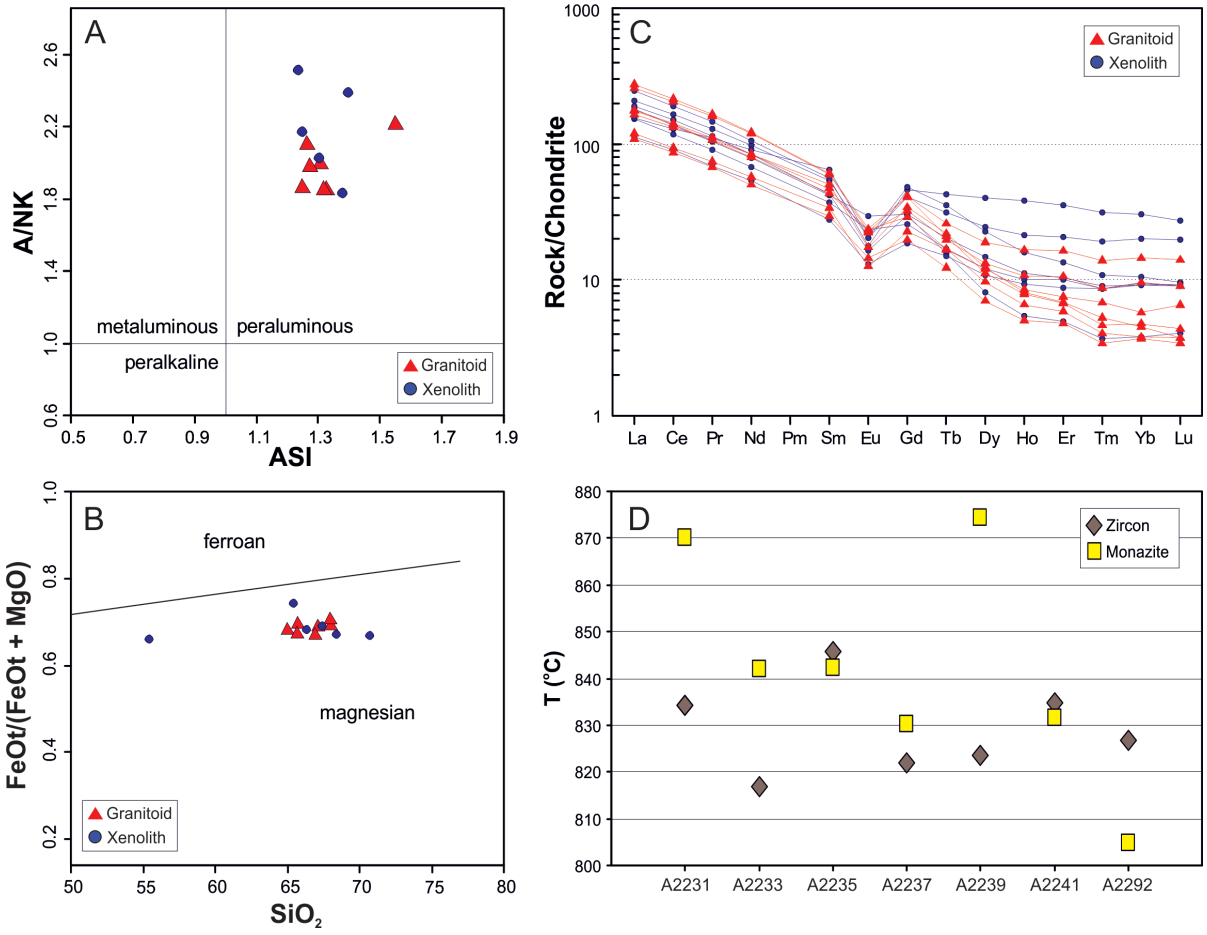

Figure 3. Chemical composition of seven granitoid-xenolith pairs from the Vaasa batholith in (A) ASI (Aluminum Saturation Index) vs. A/NK (Agpaitic Index), samples A2234 and A2293 fall outside the plotting area, both are peraluminous, (B) SiO_2 vs. FeOt/(FeOt + MgO) (Frost et al., 2001), magnesian xenolith sample A2234 falls outside the plotting area, and (C) Chondrite-normalized (Boynton, 1984) REE diagram. (D) shows zircon (Watson & Harrison, 1983) and monazite (Montel, 1993) saturation temperatures for the seven granitoids analyzed (see also Table 3).

5. Discussion

Kotilainen et al. (2016) provided a model for the spatial correlation of U–Pb zircon ages throughout the Vaasa batholith. Overall, U–Pb ages of zircon from samples near the border of the batholith are older than ages of those in the inner parts. Three xenolith samples, which contain neoformed and recrystallized zircon coeval with their host granitoids, are situated in the same area closest to the center of the batholith. In this work, we expand the spatial correlation of U–Pb ages across the Vaasa batholith utilizing the new monazite U–Pb data. In Fig. 4 our new Pb–Pb monazite ages and the U–Pb zircon ages published by Suikkanen et al. (2014) and Kotilainen et al. (2016), and U–Pb monazite ages of Alviola et al. (2001) and Sipilä et al. (2008) are shown relative to their distance to the approximated batholith border. The following observations can be made regarding the significance and interrelations of the monazite and zircon ages:

– Age differences between zircon and monazite in an individual granitoid vary from 9 to 18 Ma (face values) or from 3 to 9 Ma (errors considered) (Table 1).

– The samples show decreasing zircon and monazite age trends towards the interior of the batholith.
– The U–Pb monazite ages of Alviola et al. (2001) and Sipilä et al. (2008) are in good agreement with both the monazite data of this paper and the spatial correlation regarding the border of the batholith.
– The U–Pb zircon data of Suikkanen et al. (2014) correlate well with the distance from the batholith border. The ages are, however, systematically younger than the ages of Kotilainen et al. (2016).

Note also that when the results of Suikkanen et al. (2014) are compared to the nearest granitoid sample analyzed by Kotilainen et al. (2016) (A2176 vs. A2298, A2178 vs. A2231, and A2180 vs. A2292, respectively; see locations in Fig. 1), the ages are identical within the analytical error.

The closure temperatures of the U–Pb system in monazite and zircon vary and are dependent on several factors. Recent studies have shown that closure temperatures for Pb diffusion may be very high (> 900 °C) in both zircon and monazite (e.g., Lee et al., 1997; Cherniak & Watson, 2001; Cherniak et al., 2004). If both closure temperatures are so high, it would be difficult to explain the ~10 m.y. difference between the zircon and monazite ages in the Vaasa batholith. One possibility is that the earlier studies of monazite closure temperatures with considerably lower values of 700–750 °C (Spear & Parrish, 1996; Dahl, 1997; Smith & Giletti, 1997) apply better to the monazites in this study. Another possibility for the established age difference is late saturation of monazite in the melt. Rapp et al. (1987) investigated monazite stability in water-saturated peraluminous to metaluminous granitic melts. For peraluminous granitic magma, monazite saturation concentrations were 360 ppm, 200 ppm and 105 ppm total LREE (La–Sm, Gd) at 850 °C, 800 °C, and 750 °C, respectively. Our data from the Vaasa batholith indicate LREE concentrations between 152–375 ppm (Table 3), and corresponding monazite saturation temperatures (Montel, 1993) between 805 °C and 874 °C (Fig. 3D). Zircon saturation temperatures (Watson & Harrison, 1983) show considerably less variation, ranging from 817 °C to 846 °C (Fig. 3D). No geographical trends can be easily traced for the temperature variations. Moreover, some doubt has been cast over the applicability of these methods in peraluminous granitoids (cf. Clemens, 2003). Because of documented zircon inheritance (Kotilainen et al. 2016), the obtained saturation temperatures should be treated as provisional. These temperatures do, however, indicate that the granitoid melts of the Vaasa batholith were comparatively hot. Because pre-existing monazite in metapelites is not expected to survive melting at 760–780 °C in 5 kbar (Yakymchuk & Brown, 2014), it is highly probable that all monazite was crystallized after melting. In fact, the texture and habit of the examined monazites are magmatic rather than metamorphic: metamorphic monazite is usually pale and translucent and depleted of U, whereas monazite of Vaasa is dark yellow and contains considerable amounts of U.

It thus seems that in the case of the Vaasa batholith, monazite was crystallized at lower temperatures than zircon. Slow cooling of the batholith (from the margin towards the center of the batholith) could explain the observed age difference. It should be noted that the experiments of e.g. Cherniak et al. (2004), which imply ~900 °C closure temperatures for monazites, dealt with relatively fast cooling only, whereas slower cooling typically leads to lower closure temperatures (e.g., Suzuki et al. 1994). In view of the fact that zircon throughout the Vaasa batholith crystallized within a rather short time window (Kotilainen et al., 2016), the gap to monazite ages may seem rather large. For comparison, in the high-grade terranes in southern Finland, granitic rocks tend to display simultaneous zircon and monazite crystallization (Kurhila et al., 2005, 2011; Mouri et al., 2005; Baltybaev et al., 2006).

Observations from smaller granitoid-migmatite complexes, which in many ways resemble the Vaasa complex, imply slow cooling rates from

Table 3. Whole-rock geochemical data on seven granitoid-xenolith pairs from the Vaasa batholith

	LABTIUM OY												U.S. GEOLOGICAL SURVEY			
	Susivuori		Haudankalliot		Saarineva		Hanhimäki		Tallmossen		Långbådan		Frakaninkalliot			
	grano-diorite	xenolith	granite	xenolith	granite	xenolith	granite	xenolith	quartz monzonite	xenolith	grano-diorite	xenolith	granite	xenolith		
	A2231	**A2232**	**A2233**	**A2234**	**A2235**	**A2236**	**A2237**	**A2238**	**A2239** (a)	**A2240**	**A2241**	**A2242**	**A2292**	**A2293**	**unit**	**method**
SiO_2	68.0	55.4	65.7	45.1	66.9	70.7	67.1	68.4	65.7	67.4	67.9	65.4	65.0	66.3	%	XRF
TiO_2	0.82	0.89	0.80	1.27	0.68	0.77	0.70	0.70	0.86	1.00	0.79	1.51	0.70	0.61	%	XRF
Al_2O_3	15.7	20.5	16.2	23.1	16.6	13.7	15.9	15.0	16.95	14.0	15.6	15.3	15.5	14.2	%	XRF
Fe_2O_3 t	4.54	8.15	5.97	14.2	4.56	5.16	6.07	5.39	5.12	7.52	5.11	6.63	6.04	6.05	%	XRF
MnO	0.04	0.08	0.06	0.20	0.04	0.06	0.06	0.05	0.07	0.12	0.04	0.07	0.04	0.13	%	XRF
MgO	1.83	3.77	2.33	6.15	2.02	2.31	2.46	2.40	2.24	3.06	1.92	2.08	2.54	2.54	%	XRF
CaO	2.33	2.07	2.4	1.66	2.07	2.09	1.77	3.48	2.97	2.31	2.59	3.18	1.94	4.75	%	XRF
Na_2O	2.91	3.21	2.82	1.90	3.08	2.65	2.32	2.52	3.32	2.36	3.41	2.76	2.91	1.26	%	XRF
K_2O	3.37	5.45	3.23	4.18	3.62	2.23	3.11	1.68	2.42	1.83	2.09	2.33	3.34	1.46	%	XRF
P_2O_5	0.07	0.07	0.08	0.06	0.13	0.06	0.12	0.13	0.06	0.04	0.27	0.48	0.20	0.14	%	XRF
Cr_2O_3	n.a.	n.a.	n.a	n.a.	n.a.	n.a.	n.a.	n.a.	n.a.	n.a.	n.a.	n.a.	0.02	0.01	%	XRF
LOI	n.a.	n.a.	n.a	n.a.	n.a.	n.a.	n.a.	n.a.	n.a.	n.a.	n.a.	n.a.	1.29	1.8	%	Combustion
Total	**99.60**	**99.60**	**99.59**	**97.83**	**99.70**	**99.72**	**99.61**	**99.75**	**99.66**	**99.64**	**99.71**	**99.73**	**99.52**	**99.25**	%	
Sc	11.2	22.2	17.2	46.1	10.8	13.0	13.7	16.3	17.8	31.8	8.84	19.6	11	16	ppm	ICP-MS
V	85.3	168	122	266	99.6	110	87.0	139	143	175	74.6	75.8	96	100	ppm	ICP-MS
Cr	73.2	154	99.0	266	65.7	82.0	81.1	105	87.6	182	57.8	53.2	80	80	ppm	ICP-MS
Co	29.1	27.2	31.8	43.0	29.3	28.5	26.8	37.7	31.9	39.7	25.6	28.7	30.1	34.6	ppm	ICP-MS
Ni	22.2	49.9	42.2	83.9	29.1	24.2	34.0	42.4	36.7	35.7	24.7	21.4	42	42	ppm	ICP-MS
Cu	21.9	16.1	42.9	64.9	24.1	6.68	31.6	29.5	37.8	19.6	25.6	23.4	26	28	ppm	ICP-MS
Zn	103	142	119	211	83.7	94	107	103	88.2	115	89.3	113	110	98	ppm	ICP-MS
Y	13.6	21.4	20.0	44.4	11.4	9.6	8.6	17.8	30.2	72.1	14.4	27.6	18.3	20.8	ppm	ICP-MS
Zr (b)	178	112	147	113	196	144	129	177	164	212	180	197	219	202	ppm	XRF (Labtium), ICP-MS (USGS)
Nb (b)	<5	<5	<5	<5	<5	6	7	<5	<5	<5	6	12	19	11	ppm	XRF (Labtium), ICP-MS (USGS)
Mo	0.97	<0.5	1.75	1.07	0.75	<0.5	1.04	0.54	0.86	0.53	0.76	0.86	<2	<2	ppm	ICP-MS
Cd	0.48	0.47	0.53	0.73	0.29	0.33	0.27	0.36	0.61	0.79	0.38	0.50	<0.2	0.3	ppm	ICP-MS
Li	10.0	29.7	9.74	91.5	42.0	35.9	15.1	16.4	19.7	18.8	80.6	105	50	50	ppm	ICP-MS
Be	1.92	5.03	2.01	17.0	2.07	0.65	8.20	1.24	0.86	0.55	2.61	1.40	<5	<5	ppm	ICP-MS
Hf	4.12	3.24	2.50	2.69	3.13	3.94	2.58	4.02	2.84	4.45	3.65	4.59	6	5	ppm	ICP-MS
Rb	148	212	156	249	166	142	160	85.6	88.7	84.0	153	171	184	91.3	ppm	ICP-MS
Sr	249	294	245	208	298	220	164	310	297.5	219	209	233	174	183	ppm	ICP-MS
Ba	896	1560	751	747	820	417	563	377	597	417	192	159	388	110	ppm	ICP-MS
Ga (b)	18	20	19	28	15	<15	19	<15	<15	<15	20	16	23	19	ppm	XRF (Labtium), ICP-MS (USGS)
Tl	1.51	2.21	1.33	2.31	1.14	1.02	1.19	0.68	1.2	1.18	0.96	1.15	1	0.6	ppm	ICP-MS
As	0.74	<0.5	0.77	0.59	4.10	<0.5	1.29	<0.5	0.82	<0.5	4.94	1.42	<30	<30	ppm	ICP-MS

Table 3 (continued)

	Susivuori		Haudankalliot		Saarineva		Hanhimäki		Tallmossen		Långbådan		Frakaninkalliot			
	grano-diorite	xenolith	granite	xenolith	granite	xenolith	granite	xenolith	quartz monzonite	xenolith	grano-diorite	xenolith	granite	xenolith		
	A2231	**A2232**	**A2233**	**A2234**	**A2235**	**A2236**	**A2237**	**A2238**	**A2239** (a)	**A2240**	**A2241**	**A2242**	**A2292**	**A2293**	**unit**	**method**
Sn	<2	<2	<2	<2	<2	<2	<2	<2	<2	<2	2.76	2.56	2	1	ppm	ICP-MS
Sb	<0.1	<0.1	<0.1	<0.1	0.13	0.1	<0.1	<0.1	<0.1	<0.1	0.18	0.16	<0.1	<0.1	ppm	ICP-MS
Bi	0.15	0.12	0.14	0.18	0.26	0.11	0.15	0.14	0.15	0.15	0.22	0.21	0.1	0.1	ppm	ICP-MS
La	79.7	56.4	55.3	64.5	54.5	58.8	33.8	47.8	85.5	77.1	51.0	48.0	37.2	35.1	ppm	ICP-MS
Ce	166	111	115	134	112	121	69.7	95.5	173.5	154	108	105	75.5	72.8	ppm	ICP-MS
Pr	19.6	12.8	13.6	15.8	13.0	14.0	8.27	11.0	20.2	17.8	13.1	13.5	9.07	8.44	ppm	ICP-MS
Nd	72.0	47.4	50.6	58.5	48.0	50.5	30.0	40.7	72.9	63.5	50.5	54.5	34.3	32	ppm	ICP-MS
Sm	11.7	8.15	9.17	10.5	8.44	8.33	5.76	7.21	11.9	10.9	9.78	12.6	6.6	5.4	ppm	ICP-MS
Eu	1.67	2.18	1.63	1.49	1.71	1.21	1.06	1.73	1.74	1.31	1.27	1.50	0.92	0.96	ppm	ICP-MS
Gd	10.5	7.81	8.31	10.6	7.49	7.77	5.10	6.61	10.75	12.0	8.87	12.4	5.89	4.83	ppm	ICP-MS
Tb	0.99	0.96	0.93	1.48	0.80	0.74	0.58	0.80	1.23	2.01	1.04	1.68	0.79	0.71	ppm	ICP-MS
Dy	3.61	4.73	4.26	7.88	3.10	2.62	2.24	3.86	6.09	13.0	3.96	7.25	3.87	3.5	ppm	ICP-MS
Ho	0.56	0.80	0.77	1.52	0.47	0.39	0.36	0.72	1.19	2.73	0.58	1.14	0.61	0.67	ppm	ICP-MS
Er	1.40	2.17	2.22	4.36	1.23	1.03	1.00	2.09	3.43	7.39	1.43	2.83	1.57	1.84	ppm	ICP-MS
Tm	0.15	0.29	0.28	0.62	0.13	0.12	0.11	0.28	0.45	1.01	0.17	0.35	0.22	0.28	ppm	ICP-MS
Yb	0.99	1.90	1.99	4.22	0.79	0.79	0.77	1.96	3.02	6.33	0.94	2.19	1.2	1.9	ppm	ICP-MS
Lu	0.14	0.29	0.29	0.64	0.12	0.13	0.11	0.29	0.45	0.88	0.12	0.31	0.21	0.3	ppm	ICP-MS
Th	35.1	20.5	24.1	23.9	19.3	22.3	13.9	16.1	26.1	25.3	17.6	13.1	14.3	12.9	ppm	ICP-MS
U	1.82	1.79	2.21	2.39	3.19	2.12	2.26	3.06	2.31	1.80	3.07	3.42	2.55	2.82	ppm	ICP-MS
Pb	26.1	35.4	23.3	18.0	24.1	14.6	15.5	16.3	20.8	15.1	16.1	12.3	15	7	ppm	ICP-MS
Sat temp Zirc (c)	834		817		846		822		823		835		827		°C	
Sat temp Mnz (d)	870		842		842		830		874		832		805		°C	

(a) Average of two analyses

(b) Zr, Nb, and Ga were analyzed as oxide-% by XRF in Labtium, and recalculated to ppm

(c) Saturation temperature according to Watson & Harrison (1983)

(d) Saturation temperature according to Montel (1993), with 5 % water content

6 °C per m.y. (Morfin et al., 2013) to 3 °C per m.y. (Petitgirard et al., 2009), and sustained continuous anatexis for tens of m.y. (Montero et al., 2004). Also, Gordon et al. (2009) suggested that the Valhalla migmatite complex in Canada maintained an elevated temperature, sufficient for an open U–Pb system in monazite, in excess of 7 m.y. Furthermore, Parrish & Tirrul (1989) have shown that, after emplacement, monazites in the Baltoro granite, northwest Himalaya, remained near the closure temperature for several millions of years. Morfin et al. (2013) suggested that slow cooling of the Opinaca Subprovince resulted from the combined effect of high concentration of heat-producing elements and latent heat of crystallization. The aeroradiometric Th map of the Vaasa complex (Fig. 5) shows that the highest Th contents are in the granite areas, obviously reflecting the abundance of monazite, which is the main host mineral for Th. Potassium and U are also enriched in the same area as Th, indicating high radiogenic heat production in the western part of the complex. However, the U–Pb ages of monazites are, within error limits, essentially the same throughout the Vaasa complex (Fig. 5). On the other hand, monazite and zircon ages from samples within the batholith show overall decreasing trends from the marginal to the central part of the batholith (Fig. 4).

In the light of our new U–Pb monazite ages and pre-existing geochronological data, we conclude that the granitoids and the metasedimentary rocks of the Vaasa batholith record slow cooling, especially in the central part of the batholith. Overall, the currently exposed central part of the batholith probably represents a relatively deep section through the Paleoproterozoic middle crust, and thus offers an *a priori* window to the midcrustal processes that occurred at the culmination stage of the Svecofennian orogeny in the central part of the Svecofennian orogen.

6. Conclusion

Subsequent to the ~1875 Ma culmination of the Svecofennian orogeny, profuse anatexis and crystallization of resultant, crustally derived peraluminous melts formed the Vaasa granite batholith. After having reached the solidus, the batholith experienced a prolonged cooling event, originally proposed by Kotilainen et al. (2016) based on U–Pb zircon ages from the batholith center that are 5–10 m.y. younger than those in the batholith margin. This hypothesis is reinforced by our new U–Pb monazite ages that are younger than the zircon ages of the respective granitoid samples.

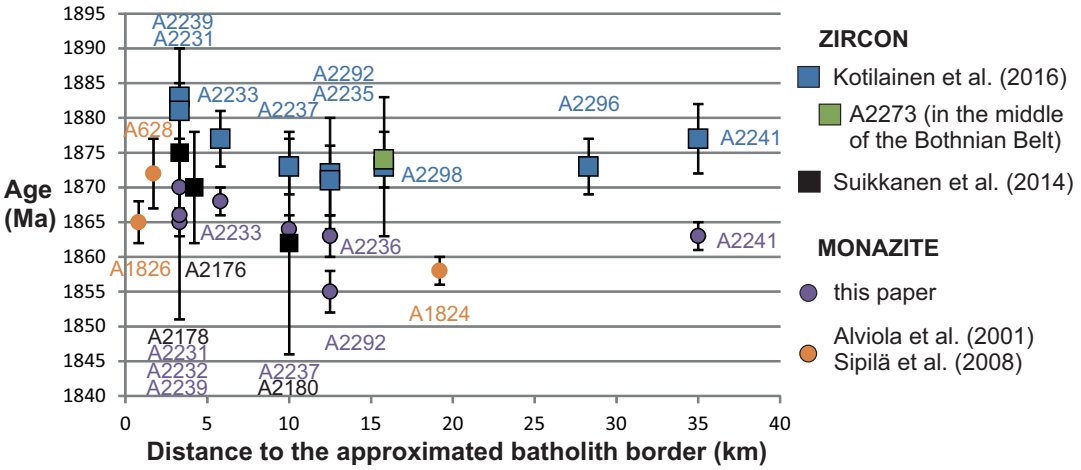

Figure 4. The U–Pb zircon ages of the granitoids (Suikkanen et al., 2014; Kotilainen et al., 2016) and the monazite ages of the Vaasa batholith (this study; Alviola et al., 2001; Sipilä et al., 2008) compared to the distance from the approximated batholith border (see Fig. 1A in Kotilainen et al., 2016).

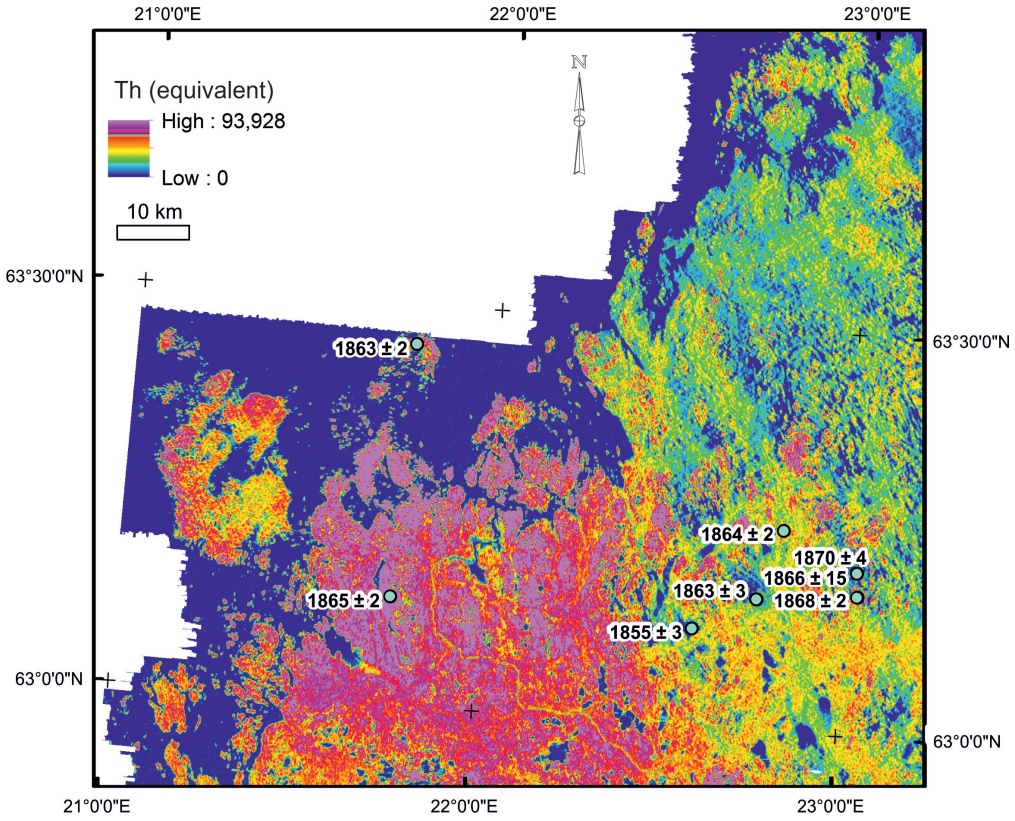

Figure 5. Aeroradiometric Th map of the Vaasa complex, compiled from the database of the Geological Survey of Finland (GTK). Sample sites for granitoids and xenoliths from which monazite U-Pb data were acquired are shown with respective monazite U-Pb ages.

Acknowledgements

This study was funded by the MIDCRUST consortium (Annakaisa Korja, P.I.; O.T. Rämö, co-P.I.; Academy of Finland project 139035), the Finnish National Doctoral Program in Geology, the Doctoral Program in Geosciences, University of Helsinki, and the Finnish Cultural Foundation (South Ostrobothnia Regional Fund). Leena Järvinen and Arto Pulkkinen from the GTK are thanked for assistance in the isotope dilution work, Mirja Saarinen for heavy liquid separations, and Pekka Simelius for help while milling the samples. Insightful reviews of the original submission by Perttu Mikkola and Thomas Zack and comments from the Editor-in-Chief (Jussi Heinonen) improved the manuscript. Discussions with Francis Chopin and Seija Kultti are sincerely appreciated.

References

Alviola, R., Mänttäri, I., Mäkitie, H. & Vaasjoki, M., 2001. Svecofennian rare-element granitic pegmatites of the Ostrobothnia region, western Finland: their metamorphic environment and time of intrusion. Geological Survey of Finland, Special Paper 30, 9–29.

Baltybaev, Sh.K., Levchenkov, O.A., Levsky, L.K., Eklund, O. & Kilpeläinen, T., 2006. Two metamoprhic stages in the Svecofennian domain: Evidence from the isotopic geochronological study of the Ladoga and Sulkava metamorphic complexes. Petrology 14, 247–261. http://dx.doi.org/10.1134/S0869591106030039

Bergman, S., Högdahl, K., Nironen, M., Ogenhall, E., Sjöström, H., Lundqvist, L. & Lahtinen, R., 2008. Timing of Paleoproterozoic intra-orogenic sedimentation in the central Fennoscandian Shield; evidence from detrital zircon in metasandstone. Precambrian Research 161, 231–249. http://dx.doi.org/10.1016/j.precamres.2007.08.007

Boynton, W.V., 1984. Cosmochemistry of the rare earth elements: meteorite studies. In: Henderson, P. (Ed.), Rare

Earth Element Geochemistry. Elsevier B.V., Amsterdam, 63–114.

Cherniak, D.J. & Watson, E.B., 2001. Pb diffusion in zircon. Chemical Geology 172, 5–24. http://dx.doi.org/10.1016/S0009-2541(00)00233-3

Cherniak, D.J., Watson, E.B., Grove, M. & Harrison, T.M., 2004. Pb diffusion in monazite: A combined RBS/SIMS study. Geochimica et Cosmochimica Acta 68, 829–840. http://dx.doi.org/10.1016/j.gca.2003.07.012

Claesson, S., Huhma, H., Kinny, P.D. & Williams, I.S., 1993. Svecofennian detrital zircon ages–implications for the Precambrian evolution of the Baltic Shield. Precambrian Research 64, 109–130. http://dx.doi.org/10.1016/0301-9268(93)90071-9

Clemens, J.D., 2003. S-type granitic magmas; petrogenetic issues, models and evidence. Earth-Science Reviews 61, 1–18. http://dx.doi.org/10.1016/S0012-8252(02)00107-1

Copeland, P., Parrish, R.R. & Harrison, T.M., 1988. Identification of inherited radiogenic Pb in monazite and implications for U–Pb systematics. Nature 333, 760–763. http://dx.doi.org/10.1038/333760a0

Dahl, P.S., 1997. A crystal-chemical basis for Pb retention and fission-track annealing systematics in U-bearing minerals, with implications for geochronology. Earth and Planetary Science Letters 150, 277–290. http://dx.doi.org/10.1016/S0012-821X(97)00108-8

Frost, B.R., Barnes, C.G., Collins, W.J., Arculus, R.J., Ellis, D.J. & Frost, C.D., 2001. A geochemical classification for granitic rocks. Journal of Petrology 42, 2033-2048.

Gordon, S.M., Grove, M., Whitney, D.L., Schmitt, A.K. & Teyssier, C., 2009. Time–temperature–fluid evolution of migmatite dome crystallization: Coupled U–Pb age, Ti thermometry, and O isotopic ion microprobe depth profiling of zircon and monazite. Chemical Geology 262, 186–201. http://dx.doi.org/10.1016/j.chemgeo.2009.01.018

Hölttä, P., 2013. Svecofennian metamorphism in Pohjanmaa, western Finland. Geological Survey of Finland, Report of Investigation 198, 62–64.

Huhma, H., 1986. Sm-Nd, U-Pb and Pb-Pb isotopic evidence for the origin of the Early Proterozoic Svecocarelian crust in Finland. The Geological Survey of Finland Bulletin 337, 48 p.

Huhma, H., Claesson, S., Kinny, P.D. & Williams, I.S., 1991. The growth of Early Proterozoic crust: New evidence from Svecofennian detrital zircon. Terra Nova 3, 175–179. http://dx.doi.org/10.1111/j.1365-3121.1991.tb00870.x

Kähkönen, Y., 2005. Svecofennian supracrustal rocks. In: Lehtinen, M., Nurmi, P.A. & Rämö, O.T. (Eds.), Precambrian Geology of Finland – Key to the evolution of the Fennoscandian Shield. Elsevier B.V., Amsterdam, 343–406.

Korja, A. & Heikkinen, P., 2005. The accretionary Svecofennian orogen – insight from the BABEL profiles. Precambrian Research 136, 241–268. http://dx.doi.org/10.1016/j.precamres.2004.10.007-

Kotilainen, A.K., Mänttäri, I., Kurhila, M., Hölttä, P. & Rämö, O.T., 2016. Evolution of a Palaeoproterozoic giant magmatic dome in Finnish Svecofennian; New insights from U–Pb geochronology. Precambrian Research 272, 39–56. http://dx.doi.org/10.1016/j.precamres.2015.10.023

Kouvo, O. & Tilton, G., 1966. Mineral ages from the Finnish Precambrian. Journal of Geology 74, 421–442.

Krogh, T.E., 1973. A low-contamination method for hydrothermal decomposition of U and Pb for isotopic age determinations. Geochimica et Cosmochimica Acta 37, 485–494. http://dx.doi.org/10.1016/0016-7037(73)90213-5

Krogh, T.E., 1982. Improved accuracy of U–Pb zircon ages by the creation of more concordant systems using an air abrasion technique. Geochimica et Cosmochimica Acta 46, 637–649. http://dx.doi.org/10.1016/0016-7037(82)90165-X

Krohe A. & Wawrzenitz, N., 2000. Domainal variations of U–Pb monazite ages and Rb–Sr whole-rock dates in polymetamorphic paragneisses (KTB Drill Core, Germany): influence of strain and deformation mechanism on isotope systems. Journal of Metamorphic Geology 18, 271–291. http://dx.doi.org/10.1046/j.1525-1314.2000.00255.x

Kurhila, M., Vaasjoki, M., Mänttäri, I., Rämö, T. & Nironen, M., 2005. U-Pb ages and Nd isotope characteristics of the late orogenic migmatizing microcline granites in southwestern Finland. Bulletin of the Geological Society of Finland 77, 105–127.

Kurhila, M., Mänttäri, I., Vaasjoki, M., Rämö, O.T. & Nironen, M., 2011. U/Pb geochronological constraints of the late Svecofennian leucogranites of Southern Finland. Precambrian Research 190, 1–24. http://dx.doi.org/10.1016/j.precamres.2011.07.008

Lahtinen, R., Huhma, H. & Kousa, J., 2002. Contrasting source components of the Paleoproterozoic Svecofennian metasediments: Detrital zircon U–Pb, Sm–Nd and geochemical data. Precambrian Research 116, 81–109. http://dx.doi.org/10.1016/S0301-9268(02)00018-9

Lahtinen, R., Korja, A. & Nironen, M., 2005. Paleoproterozoic tectonic evolution. In: Lehtinen, M., Nurmi, P.A., Rämö, O.T. (Eds.), Precambrian Geology of Finland – Key to the evolution of the Fennoscandian Shield. Elsevier B.V., Amsterdam, 481–531.

Lahtinen, R., Huhma, H., Kähkönen, Y. & Mänttäri, I., 2009. Paleoproterozoic sediment recycling during multiphase orogenic evolution in Fennoscandia, the Tampere and Pirkanmaa Belts, Finland. Precambrian Research 174, 310–336. http://dx.doi.org/10.1016/j.precamres.2009.08.008

Lee, J.K.W., Williams, I.S. & Ellis, D.J., 1997. Pb, U and Th diffusion in natural zircon. Nature 390, 159–162. http://dx.doi.org/10.1038/36554

Lehtonen, M.I., Kujala, H., Kärkkäinen, N., Lehtonen, A., Mäkitie, H., Mänttäri, I., Virransalo, P. & Vuokko, J., 2005. Etelä-Pohjanmaan liuskealueen kallioperä. Geologian tutkimuskeskus, Tutkimusraportti 158, 125 p.

Ludwig, K.R., 1993. PbDat. A computer program for processing Pb-U-Th isotope data. Version 1.24. United States Geological Survey open-file report 88-542. Revision of June 22, 1993.

Ludwig, K.R., 2012. Isoplot 3.75. A geochronological toolkit for Microsoft Excel. Berkeley Geochronological Center Special Publication No 5.

Lundqvist, T. & Autio, S. (Eds.), 2000. Description to the bedrock map of central Fennoscandia (Mid-Norden). Geological Survey of Finland, Special Paper 28, 176 p.

Mäkitie, H., Kärkkäinen, N., Lahti, S.I. & Lehtonen, M.I., 1999. Chemical and modal compositions of granitoids in three different geological units, South-Pohjanmaa, western Finland. Geological Survey of Finland Special Paper 27, 7–19.

Mäkitie, H., 2001. Eastern margin of the Vaasa Migmatite Complex, Kauhava, western Finland: preliminary petrography and geochemistry of the diatexites. Bulletin of the Geological Society of Finland 73, 35–46.

Mäkitie, H., Sipilä, P., Kujala, H., Lindberg, A. & Kotilainen, A., 2012. Formation mechanism of the Vaasa Batholith in the Fennoscandian Shield: petrographic and geochemical constraints. Bulletin of the Geological Society of Finland 84, 141–166.

Montel, J.-M., 1993. A model for monazite/melt equilibrium and application to the generation of granitic magmas. Chemical Geology 110, 127–146. http://dx.doi.org/10.1016/0009-2541(93)90250-M

Montero, P., Bea, F., Zinger, T.F., Scarrow, J.H., Molina, J.F. & Whitehouse, M., 2004. 55 million years of continuous anatexis in Central Iberia: single-zircon dating of the Peña Negra Complex. Journal of the Geological Society of London 161, 255–263. http://dx.doi.org/10.1144/0016-764903-024

Morfin, S., Sawyer, E.W. & Bandyayera, D., 2013. Large volumes of anatectic melt retained in granulite facies migmatites; an injection complex in northern Quebec. Lithos 168–169, 200–218. http://dx.doi.org/10.1016/j.lithos.2013.02.007

Mouri, H., Väisänen, M., Huhma, H. & Korsman, K., 2005. Sm-Nd garnet and U-Pb monazite dating of high-grade metamorphism and crustal melting in the West Uusimaa area, southern Finland. GFF 127, 123–128. http://dx.doi.org/10.1080/11035890501272123

Nironen, M., 1997. The Svecofennian Orogen: a tectonic model. Precambrian Research 86, 21–44. http://dx.doi.org/10.1016/S0301-9268(97)00039-9

Noble, S.R. & Searle, M.P., 1995. Age of crustal melting and leucogranite formation from U-Pb zircon and monazite dating in western Himalaya, Zanskar, India. Geology 23, 1135–1138. http://dx.doi.org/10.1130/0091-7613(1995)023<1135:AOCMAL>2.3.CO;2

Parrish, R.R., 1990. U–Pb dating of monazite and its application to geological problems. Canadian Journal of Earth Sciences 27, 1431–1450. http://dx.doi.org/10.1139/e90-152

Parrish, R.R. & Tirrul, R., 1989. U-Pb age of the Baltoro granite, northwest Himalaya, and implications for monazite U-Pb systematics. Geology 17, 1076–1079. http://dx.doi.org/10.1130/0091-7613(1989)017<1076:UPAOTB>2.3.CO;2

Patchett, P.J., Kouvo, O., Hedge, C.E. & Tatsumoto, M., 1981. Evolution of continental crust and mantle heterogeneity: Evidence from Hf isotopes. Contributions to Mineralogy and Petrology 78, 279–297. http://dx.doi.org/10.1007/BF00398923

Petitgirard, S., Vauchez, A., Egydio-Silva, M., Bruguier, O., Camps, P., Monié, P., Babinski, M. & Mondou, M., 2009. Conflicting structural and geochronological data from yhe Ibituruna quartz-syenite (SE Brazil): Effect of protracted "hot" orogeny and slow cooling rate. Tectonophysics 477, 174–196. http://dx.doi.org/10.1016/j.tecto.2009.02.039

Rapp, R.P., Ryerson, F.J. & Miller, C.F., 1987. Experimental evidence bearing on the stability of monazite during crustal anatexis. Geophysical Research Letters 14, 307–310. http://dx.doi.org/10.1029/GL014i003p00307

Rutland, R.W.R., Williams, I.S. & Korsman, K., 2004. Pre-1.91 Ga deformation and metamorphism in the Palaeoproterozoic Vammala migmatite belt, southern Finland, and implications for Svecofennian tectonics. Bulletin of the Geological Society of Finland 76, 93–140.

Sipilä, P., Kujala, H. & Torssen, M., 2008. Pre-Quaternary rocks of the Oravainen-Lapua, Alahärmä area. Geological Survey of Finland, Report of Investigation 170, 40 p.

Smith, H.A. & Giletti, B.J., 1997. Lead diffusion in monazite. Geochimica et Cosmochimica Acta 61, 1047–1055. http://dx.doi.org/10.1016/S0016-7037(96)00396-1

Spear, F.S. & Parrish, R.R., 1996. Petrology and cooling rates of the Valhalla Complex, British Columbia, Canada. Journal of Petrology 37, 733–763. http://dx.doi.org/10.1093/petrology/37.4.733

Stacey, J.S. & Kramers, J.D., 1975. Approximation of terrestrial lead isotope evolution by two stage model. Earth and Planetary Science Letters 26, 207–221. http://dx.doi.org/10.1016/0012-821X(75)90088-6

Suikkanen, E., Huhma, H., Kurhila, M. & Lahaye, Y., 2014. The age and origin of the Vaasa migmatite complex revisited. Bulletin of the Geological Society of Finland 86, 41–55.

Suzuki K., Adachi M., & Kajizuka I., 1994. Electron microprobe observations of Pb diffusion in metamorphosed detrital monazites. Earth Planetary Science Letters 128, 391–405. http://dx.doi.org/10.1016/0012-821X(94)90158-9

Teufel, S. & Heinrich, W., 1997. Partial resetting of the U–Pb isotope system in monazite through hydrothermal experiments: An SEM and U–Pb isotope study. Chemical

Geology 137, 273–281. http://dx.doi.org/10.1016/S0009-2541(96)00161-1

Townsend, K.J., Miller, C.F., D'Andrea, J.L., Ayers, J.C., Harrison, T.M. & Coath, C.D., 2000. Low temperature replacement of monazite in the Iretaba granite, Southern Nevada: geochronological implications. Chemical Geology 172, 95–112. http://dx.doi.org/10.1016/S0009-2541(00)00238-2

Vaasjoki, M., 1981. The lead isotopic composition of some Finnish galenas. Geological Survey of Finland Bulletin 316, 31 p.

Valtonen, O., 2011. Pohjanmaan kompleksin tulkinta painovoimamallinnuksen ja seismisten aineistojen avulla. M.Sc thesis, University of Helsinki. 73 p.

Vavra, G. & Schaltegger, U., 1999. Post-granulite facies monazite growth and rejuvenation during Permian to Lower Jurassic thermal and fluid events in the Ivrea Zone (Southern Alps). Contributions to Mineralogy and Petrology 134, 405–414. http://dx.doi.org/10.1007/s004100050493

Watson, E.B. & Harrison, T.M., 1983. Zircon saturation revisited: temperature and composition effects in a variety of crustal magma types. Earth and Planetary Science Letters 64, 295–304. doi:10.1016/0012-821X(83)90211-X

Williams, M.L., Jercinovic, M.J. & Terry, M.P., 1999. Age mapping and dating of monazite on the electron microprobe: Deconvoluting multistage tectonic histories. Geology 27, 1023–1026. http://dx.doi.org/10.1130/0091-7613(1999)027<1023:AMADOM>2.3.CO;2

Yakymchuk, C. & Brown, M., 2014. Behaviour of zircon and monazite during crustal melting. Journal of Geological Society, London 171, 465–479. http://dx.doi.org/10.1144/jgs2013-115